

Influence of oxygen and post deposition annealing on the electrical properties of MnPc and MnPcCl Schottky barrier devices

K. R. RAJESH, C. S. MENON

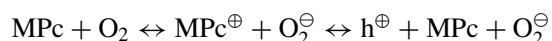
School of Pure and Applied Physics, Mahatma Gandhi University, Kottayam, Kerala-686560, India

E-mail: rajthinfilm@yahoo.co.in

Sandwich structures of manganese phthalocyanine (MnPc) and manganese phthalocyanine chloride (MnPcCl) thin films using aluminium (Al) and gold (Au) electrodes have been prepared by thermal evaporation. Device characteristics of Al/MnPc/Au and Al/MnPcCl/Au are performed and found to show rectification properties. The electrical conductivity has been measured both after exposure to oxygen for 20 days and after annealing at temperature up to 473 K. Current density-voltage characteristics under forward bias (aluminium electrode negative) are found to be due to ohmic conduction at lower voltage regions. At higher voltage regions there is space charge limited conductivity (SCLC) controlled by a discrete trapping level above the valance edge. The electrical parameters of oxygen doped and annealed samples in the ohmic and SCLC region are determined. The reverse bias curves are interpreted in terms of a transition from electrode-limited Schottky emission to the bulk-limited the Poole-Frenkel effect. The Schottky barrier parameters of oxygen doped and annealed structures of MnPc and MnPcCl are determined from the C^2 - V characteristics. © 2005 Springer Science + Business Media, Inc.

1. Introduction

Organic materials have potential advantages for use as active layers in electroluminescent displays as well as photoelectric and sensor devices, because they are easily processable in low cost and large area device fabrication. Phthalocyanines (Pc) are a class of highly stable organic compounds, which are classified as *p*-type semiconductor characterized by low mobility and low carrier concentration [1]. The conductivity of these materials depends on the gaseous environment, and thus gas sensors based on phthalocyanines have recently attracted considerable interest [2]. Oxygen is found to have a very large influence on the photovoltaic behaviour of phthalocyanine-based junctions [3]. Oxygen creates acceptor levels within the band gap of these materials. Oxygen can act as an ionization centre in the phthalocyanine lattice according to the expression



where MPc is the metal-substituted phthalocyanine and h^{\oplus} is a hole. Therefore it can favour the charge separation process upon the thermal degradation of the electronic excitation. Relatively few studies have conducted on manganese phthalocyanine chloride (MnPcCl) thin films. The object of this paper is to study the electrical conductivity of MnPc and MnPcCl sandwich structures using ohmic gold [4, 5] and blocking aluminium [6] electrodes. The effects of oxygen doping and annealing

on the conductivity properties are also investigated. These studies are capable of providing considerable insight into the charge transport mechanisms and carrier trapping in this material, and such information is of particular importance in the development of viable thin film gas sensing devices.

2. Experimental details

The MnPc and MnPcCl powder obtained from Aldrich Inc. USA are used as the source materials. Sandwich samples are prepared by thermal evaporation at a base pressure of 10^{-5} Pa. For fabricating the structures a thin layer of gold of 100 nm is first deposited as the bottom electrode. Gold is preferred as the bottom electrode because most of the aluminium-like low work function metals form an oxidizing layer, which has an effect on the Schottky behavior. Over which phthalocyanine layer is vacuum deposited. The thickness of the film is in consideration between effective Schottky behavior and shortness. The very thin layer produces 'shortness' and if the thickness is very large bulk resistance may be comparable with the depletion resistance in the lower forward bias. Finally an aluminium layer of thickness 120 nm is deposited. The thickness of the film is measured using the Tolansky's multiple beam interference technique [7]. The rates of deposition are typically 0.5 nms^{-1} . The area of each sample studied is $1.2 \times 10^{-5} \text{ m}^2$. Before evaporating the top aluminium electrode one film is kept exposed to dry air

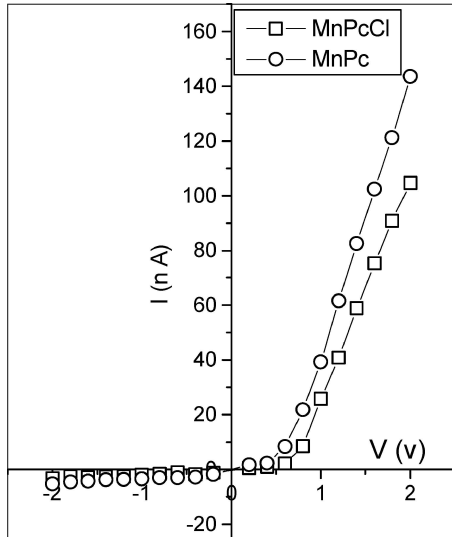


Figure 1 *I-V* characteristics of the Al/MnPc/Au and Al/MnPcCl/Au.

for 20 days and another annealed in air at 473 K for 3 h in a furnace attached to a programmable temperature controller. Sample currents are measured using a stabilized power supply and a Keithley electrometer (model No. 617). The temperature is measured using a Cr-Al thermocouple placed in close proximity to the specimen. Capacitance measurements performed using a Hioki 3532 LCR Hi-tester. To avoid contamination, measurements are performed in a subsidiary vacuum of

10^{-3} Pa. The samples are shielded from incident light to avoid photoelectric effect.

3. Results and discussions

Typical *I-V* characteristics of the Al/MnPc/Au and Al/MnPcCl/Au are shown in Fig. 1. The forward bias direction corresponds to the situation when the bottom gold electrode is positive. The space charge region is detected in the *I-V* plots by giving rise to a rectification effect. This behaviour can be explained by the low work function of Al and high work function of Au and by the *p*-type conduction of MnPc and MnPcCl.

The rectification observed is due to the blocking contact or a Schottky barrier which is formed at the Al/MnPc and Al/MnPcCl interfaces, where the conduction and valence band edges bend downward at equilibrium. The Au electrode having a high work function, $\Phi = 5.47$ [8] forms an ohmic contact with the phthalocyanine layer. The hole blocking Al contact transfer electrons from the metal to the semiconductor and due to the difference in work function reverse flow is not possible. These electrons are compensated by the holes in the semiconductor and a layer with higher thickness is formed nearer to the Al junction called depletion layer. This layer is responsible for the electric characteristics of the diode. Band structure of ohmic and Schottky contacts are shown in Fig. 2.

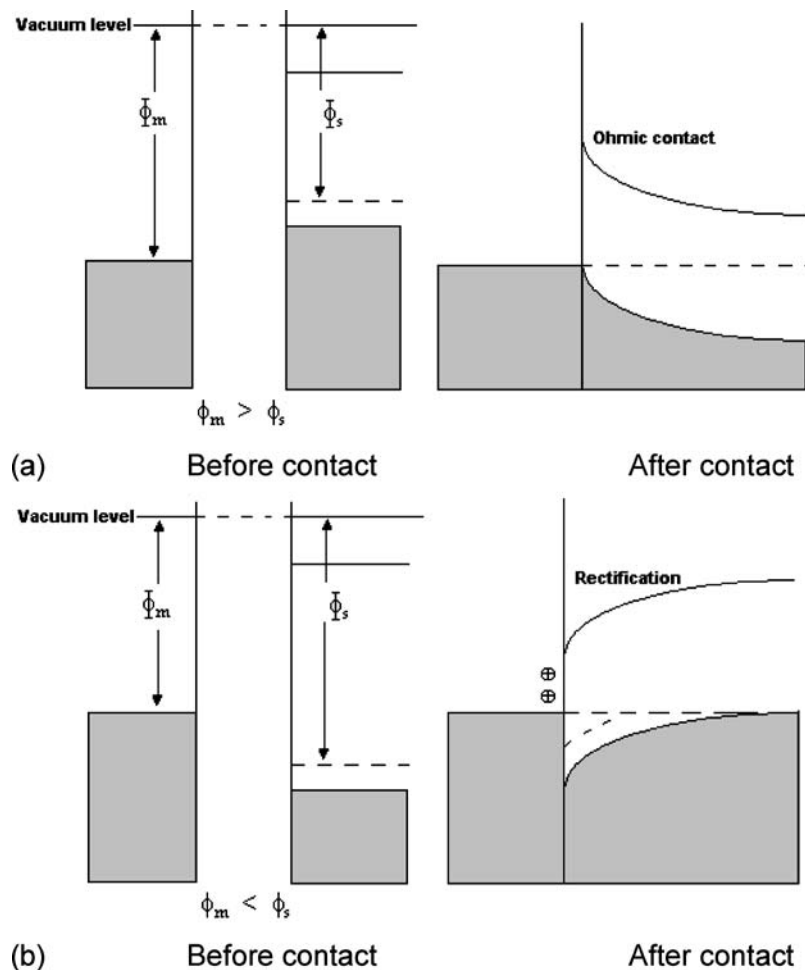


Figure 2 The band structure between a metal and a *p*-type semiconductor in a Schottky barrier device: (a) $\Phi_m > \Phi_s$ and (b) $\Phi_m < \Phi_s$.

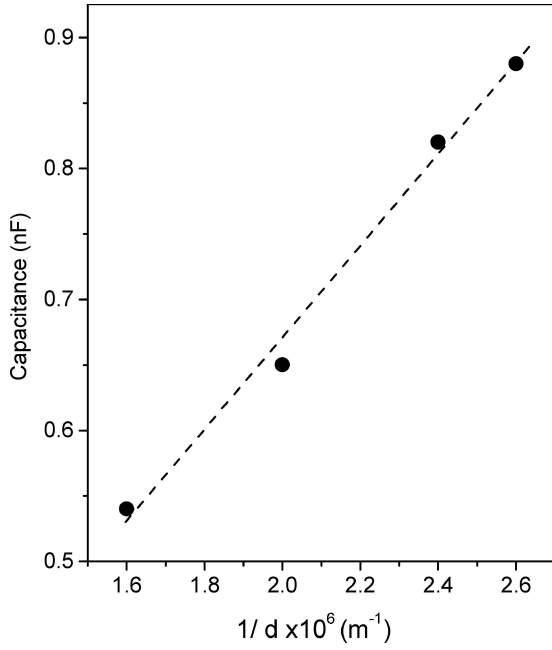


Figure 3 Capacitance versus $1/d$ for MnPcCl.

Fig. 3 shows the dependence of capacitance C on the reciprocal film thickness, $1/d$ for MnPcCl. Here the capacitance measurements are made at 1 KHz. The linearity of the plot can be analyzed in terms of the capacitance of a parallel plate capacitor

$$C = \varepsilon A/d \quad (1)$$

where ε is the permittivity of phthalocyanine layer, A is the area ($1.2 \times 10^{-5} \text{ m}^2$) and d is the thickness of the sample. The thicknesses of the samples are in the range 204–650 nm. The value of ε is estimated from Fig. 2 and found to be $3.99 \times 10^{-11} \text{ Fm}^{-1}$. From a similar procedure the value ε of is determined to be $2.89 \times 10^{-11} \text{ Fm}^{-1}$ for MnPc. The above derived values of permittivity are in good agreement with the values in the range of $2.12\text{--}4.5 \times 10^{-11} \text{ Fm}^{-1}$ for CuPc and PbPc [9–11].

Wide-ranging information about the transport mechanism through the phthalocyanine film can be obtained from the analysis of current density (J)–voltage (V) characteristics. The forward J - V characteristics of oxygen doped and annealed Al/MnPc/Au structures are shown in Fig. 4. The main feature of this figure is that the current density of O_2 doped sample is significantly higher than those for the annealed samples. This lowering indicated that the annealing process has resulted in the removal of considerable quantities of oxygen acceptor impurities [3, 12]. Fig. 5 show the plots of $\ln J$ versus $\ln V$ for the oxygen doped and annealed Al/MnPcCl/Au. In these J - V characteristics, two distinct regions can be identified. At low voltages, the slope of $\ln J$ versus $\ln V$ plot is approximately unity. These plots suggest ohmic conduction at low voltages. Assuming conduction is via holes, the current flow may be expressed in the form [13]

$$J = ep_0\mu_p(V/d) \quad (2)$$

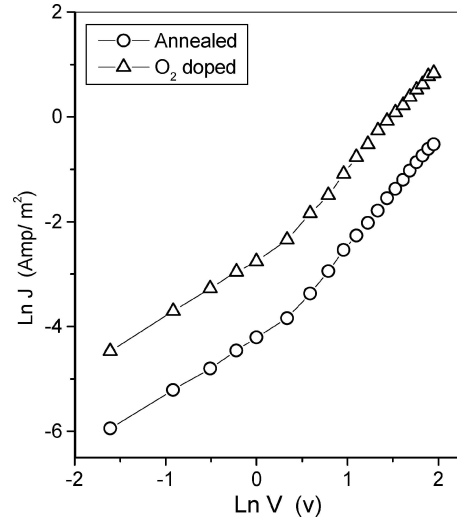


Figure 4 $\ln J$ versus $\ln V$ for Al/MnPc/Au.

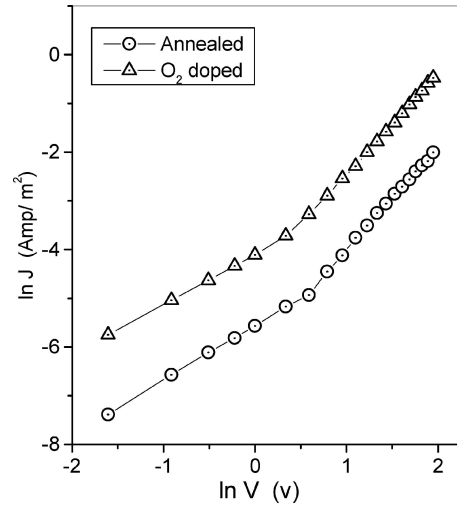


Figure 5 $\ln J$ versus $\ln V$ for Al/MnPcCl/Au.

where p_0 is the concentration of thermally generated holes in the valance band, e is the electronic charge, μ_p is the hole mobility and d is the thickness of the film. The concentration of holes at thermal equilibrium is given by

$$p_0 = N_v \exp[-(E_f - E_v)/kT] \quad (3)$$

where N_v is the effective density of state in the valance band, $(E_f - E_v)$ is the separation of Fermi level from the valance band edge, k is the Boltzmann constant and T is the absolute temperature. Now with Equation 3, the current density in the ohmic region becomes

$$J = e\mu_p N_v(V/d) \exp[-(E_f - E_v)/kT] \quad (4)$$

By plotting $\ln(J/V)$ against $1000/T$ (Fig. 6), the values of $(E_f - E_v)$ and $\mu_p N_v$ have been calculated from the slope and intercept at $1/T = 0$. Taking $N_v = 10^{27} \text{ m}^{-3}$ which correspond to one state per molecule [14], the values of $(E_f - E_v)$, μ_p and p_0 are calculated for MnPc and MnPcCl and are tabulated in Table I. These values suggest that the MnPc and MnPcCl are p -type organic

TABLE I Variation of electrical parameters in ohmic region

Sample	$E_t - E_v$ (eV)	μ_p ($m^2V^{-1}s^{-1}$)	p_0 (m^{-3})
Oxygen doped MnPc	0.58	1.67×10^{-6}	3.3×10^{18}
Annealed MnPc	0.66	1.24×10^{-6}	3.4×10^{18}
Oxygen doped MnPcCl	0.61	5.93×10^{-6}	4.0×10^{18}
Annealed MnPcCl	0.68	5.71×10^{-6}	4.2×10^{18}

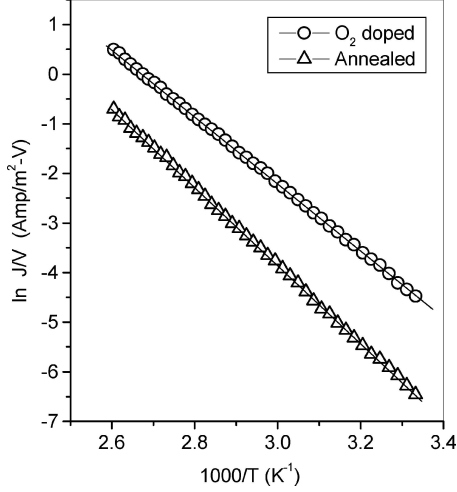


Figure 6 Typical plot of $\ln(J/V)$ versus $1000/T$ for Al/MnPc/Au.

semiconductors with low mobility and relatively high thermal activation energy.

In the higher voltage regime of the J - V characteristics (Figs 4 and 5), the slope of $\ln J$ versus $\ln V$ plot is approximately equal to 2, which shows that current is SCLC controlled by the relationship [14]

$$J = (9/8)\epsilon\mu_p\theta(V^2/d^3) \quad (5)$$

where ϵ is the permittivity of the layer and θ is the ratio of free to trapped charge carrier density or trapping factor given by [14]

$$\theta = (N_v/N_t) \exp[-(E_t - E_v)/kT] \quad (6)$$

where N_t is the total trap concentration at the energy level, $E_t - E_v$ is the activation energy of hole traps, k is the Boltzmann constant and T is the absolute temperature. Using the above expression current density in the SCLC becomes

$$J = (9/8)\epsilon\mu_p(N_v/N_t)(V^2/d^3) \exp[-(E_t - E_v)/kT] \quad (7)$$

From the above expression it is evident that $\ln(J/V^2)$ versus $1000/T$ should be a straight line. The slope and intercept at $1/T = 0$ on the current axis give $E_t - E_v$ and N_t respectively. $E_t - E_v$ and N_t , are determined from the $\ln(J/V^2)$ versus $1000/T$ plots. Fig. 7 shows $\ln(J/V^2)$ versus $1000/T$ for the oxygen doped and annealed MnPcCl thin films. Using these values in Equation 6 the trapping factor θ is estimated. The obtained values of $E_t - E_v$, N_t and θ are given in Table II. The activation energy $E_t - E_v$ decreases when the samples are annealed in air. This may be due to an in-

TABLE II Variation of electrical parameters SCLC region

Sample	$E_t - E_v$ (eV)	N_t (m^{-3})	θ
Oxygen doped MnPc	0.72	3.18×10^{21}	3.36×10^{-6}
Annealed MnPc	0.79	4.51×10^{21}	7.21×10^{-7}
Oxygen doped MnPcCl	0.62	8.53×10^{23}	4.59×10^{-8}
Annealed MnPcCl	0.71	9.64×10^{23}	5.37×10^{-7}

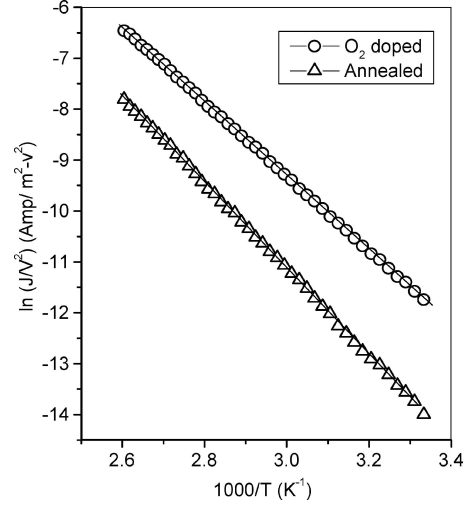


Figure 7 $\ln(J/V^2)$ versus $1000/T$ for Al/MnPcCl/Au.

trinsic activation process, which probably results from the removal of impurities during annealing process [5].

The depletion layer or space charge capacitance associated with a p - n junction or Schottky barrier is given by [15]

$$1/C^2 = 2[V_{bi} - V - (kT/e)]/e\epsilon NA^2 \quad (8)$$

where N is the effective density of donor and acceptor, A is the area, e is the electronic charge, V is the applied voltage and V_{bi} is the barrier height. Fig. 8 shows the variation of $1/C^2$ with V for oxygen doped and annealed structures of MnPcCl. It is clear that $1/C^2$ versus

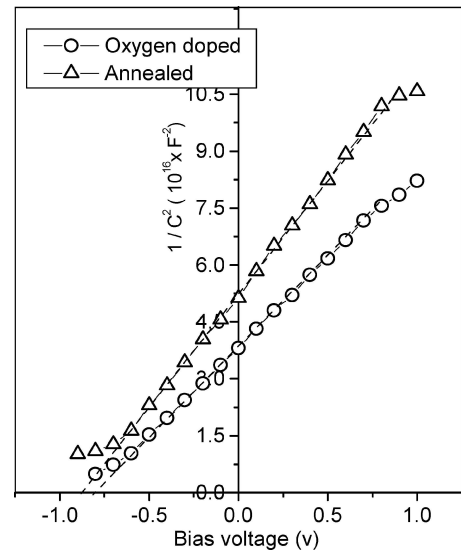


Figure 8 Variation of $1/C^2$ with V for MnPcCl.

TABLE III Variation of Schottky depletion layer parameters

Sample	N (m^{-3})	V_{bi} (eV)	W (nm)	ϕ (eV)	E_{max} (eV/ μm)	C_0 (nf)
Oxygen doped MnPc	6.51×10^{22}	0.79	66.2	1.14	23.84	5.12
Annealed MnPc	5.02×10^{22}	0.86	78.8	1.16	21.82	4.38
Oxygen doped MnPcCl	5.59×10^{22}	0.82	85.5	1.21	19.17	5.39
Annealed MnPcCl	3.98×10^{22}	0.87	101	1.27	17.16	4.56

V plots gives N [16]. According to Beth's model [17], which is commonly used when a thin insulating layer separates the semiconductor from the barrier electrode, the intercept of $1/C^2$ versus V plot with the horizontal asymptote, rather than the base line, leads to the value of V_{bi} as given by Equation 8. However, the space charge in the depletion region results from doping of phthalocyanine layer by oxygen and presumably exists as ionized oxygen. The barrier height of Schottky diode ϕ , is related to the diffusion potential, V_{bi} , by the following equation.

$$\phi = V_{\text{b}} + kT/e[1 + \ln(N_{\text{v}}/N)] \quad (9)$$

and depletion layer width (W) is given by

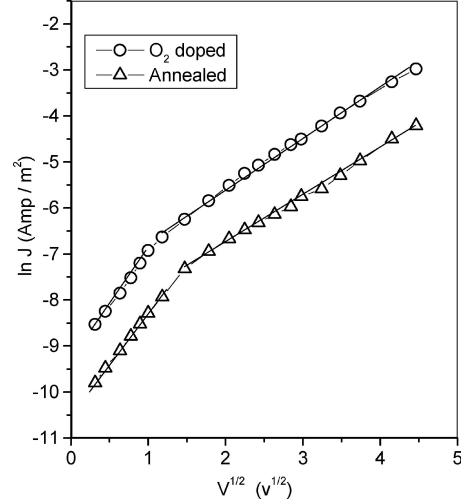
$$W = (2\varepsilon V_{\text{bi}}/eN)^{1/2} \quad (10)$$

The capacitance C_0 , at zero bias which associated with the depletion width W of high resistance, is determined for both oxygen doped and annealed structures [17]. In addition, the maximum electric field attainable in the depletion layer could be calculated from the relation

$$E_{\text{max}} = 2V_{\text{bi}}/W \quad (11)$$

The values of space charge density N , built-in potential or diffusion potential V_{bi} , depletion width W , barrier height ϕ , zero bias capacitance C_0 and maximum electric field E_{max} for MnPc and MnPcCl are listed in Table III. It can be seen that the values of N for oxygen doped samples are higher than those for the annealed samples. The higher field E_{max} , for these samples may be responsible for their high carrier concentration. It is evident that the solution to improve the performance of phthalocyanine sensing devices is to increase the acceptor concentration and to decrease the trap density. Thus oxygen is found to have a profound influence on the device characteristics of phthalocyanine based junctions.

The reverse bias current-voltage characteristics also give information about the properties of metal-semiconductor contact. The reverse current arises due to recombination of charge carriers, release of charge carriers from trap levels, barrier lowering at high electric field or leakage. Fig. 9 shows the reverse bias $\ln J$ versus $\ln V^{1/2}$ for MnPc at room temperature, which clearly yields two distinct regions. The linear sections of the curve can be interpreted in terms of either the Schottky emission or Pool-Frenkel emission.


 Figure 9 Reverse bias $\ln J - \ln V^{1/2}$ characteristics for MnPc at 300 K.

For Schottky emission the current density J is expressed as follows [18, 19],

$$J = A^* T^2 \exp(-\phi/kT) \exp(e\beta_s V^{1/2}/kTd^{1/2}) \quad (12)$$

where A^* is the effective Richardson constant, ϕ is the Schottky barrier height at the injected electrode and β_s is the Schottky field lowering constant.

For Pool-Frenkel emission, the current density is given by

$$J = J_{\text{pfo}} \exp(\beta_{\text{pf}} V^{1/2} q/kTd^{1/2}) \quad (13)$$

where β_{pf} is the Pool-Frenkel coefficient.

The theoretical values of these coefficients are given by

$$2\beta_s = \beta_{\text{pf}} = (e/\pi\varepsilon)^{1/2} \quad (14)$$

The theoretical values β_s and β_{pf} of are found to be 2.09×10^{-5} and 4.19×10^{-5} for MnPc and 1.78×10^{-5} and 3.57×10^{-5} for the MnPcCl samples. The values of β calculated from the slopes of the low voltage regions of Fig. 9 are found to be 4.22×10^{-5} and 3.66×10^{-5} for oxygen doped and annealed MnPc. For MnPcCl samples, they are 2.50×10^{-5} and 2.39×10^{-5} respectively. These values differ from both the expected Schottky and Pool-Frenkel values.

Similar behaviour has been reported previously for phthalocyanine films using aluminium-injected electrodes [5, 18–20] and is interpreted in terms of the Schottky depletion region of thickness W . Putting the theoretical value of β_s for MnPc into Equation 9, for

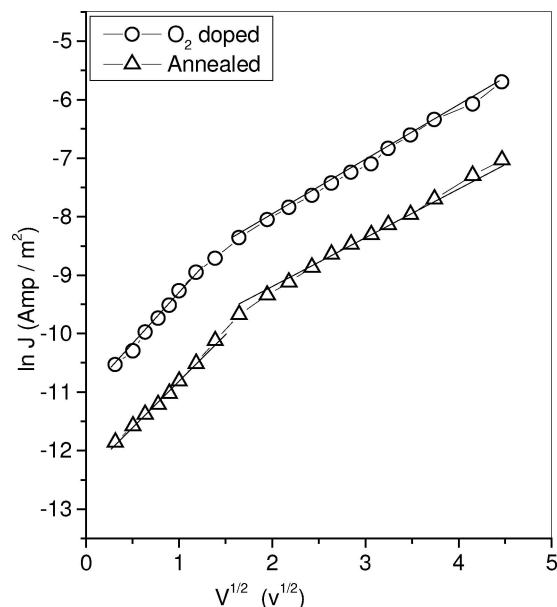


Figure 10 Reverse bias $\ln J$ - $\ln V^{1/2}$ characteristics for MnPcCl at 300 K.

oxygen doped samples the values of $W = 69.3$ nm and $\phi = 1.11$ eV and for annealed samples $W = 80.1$ nm and $\phi = 1.19$ eV have been obtained. Following a similar procedure yield, $W = 89.6$ nm and $\phi = 1.23$ eV for oxygen doped MnPcCl and $W = 104$ nm and $\phi = 1.29$ eV for the annealed MnPcCl. These values are found close to the values calculated from the C - V^2 characteristics. These results suggest that in the low field region the conduction mechanism is controlled by Schottky emission over the space charge region formed at the metal/organic semiconductor interface. At low field conduction by Schottky emission is reported in the case of ZnPc device [21].

The values of β for MnPc derived from the slopes of the high voltage sections of Fig. 9 are found to be 4.36×10^{-5} and 4.65×10^{-5} for oxygen doped and annealed samples respectively. In the case of MnPcCl (Fig. 10) these values are 3.72×10^{-5} and 3.91×10^{-5} respectively. In the higher voltage region experimental values of β for annealed samples is in close agreement with the theoretically calculated values of β_{pf} , suggesting that the conduction is bulk limited in this range. Thus it appears that the effect of annealing may improve the uniformity of electric field distribution in MnPc and MnPcCl thin films.

4. Conclusions

Current density-voltage measurements on Al/MnPc/Au and Al/MnPcCl/Au structures for both oxygen-doped and annealed samples show characteristics of typical Schottky-barrier devices. From the dependence of capacitance C on the reciprocal film thickness the

permittivity of the samples are calculated. Under forward bias, two separate regions are observed. These characteristics show ohmic conductivity at low voltages and space charge limited conductivity at higher voltages. The electrical parameters of oxygen doped and annealed samples in the ohmic and SCLC region are determined. The reverse bias curves are interpreted in terms of an electrode-limited to bulk-limited transition from Schottky emission to the Poole-Frenkel effect. Information on the thickness of the depletion region, diffusion potential, barrier height, and acceptor density of holes, can be successfully obtained by analyzing the characteristics for both oxygen-doped and annealing samples. The main conclusion obtained from these measurements is that oxygen have a large influence on the parameter values of W , ϕ and N . In general, the present results accentuate the role of oxygen doping and the existence of interfacial oxide layer in the determination of the electrical characteristics of MnPc and MnPcCl based devices.

References

1. R. D. GOULD, *Coord. Chem. Rev.* **156** (1996) 237.
2. R. A. COLLINS and K. A. MOHAMMED, *J. Physica D* **21** (1998) 154.
3. T. G. ABDEL-MALIK, *Thin Solid Films* **205** (1991) 241.
4. T. G. ABDEL-MALIK, A. A. AHMED and A. S. RIAD, *Phys. Status. Solidi (a)*, **121** (1990) 507.
5. S. GRAVANO, A. K. HASSAN and R. D. GOULD, *Int. J. Electron* **70** (1991) 477.
6. M. MARTIN, J. J. ANDRÉ and J. SIMON, *Nouv. J. Chim.* **5** (1981) 485.
7. L. I. MAISSEL and R. GLANG, "Hand Book of Thin Film Technology" (McGraw-Hill, New York, 1983).
8. MICHEL MARTIN, JEAN-JACQUES ANDRÉ and JACQUES SIMON, *J. Appl. Phys.* **54** (5) (1983) 2792.
9. A. AHMED and R. A. COLLINS, *Phys. Status Solidi (a)*, **123** (1991) 201.
10. R. D. GOULD, *Thin Solid films* **125** (1985) 63.
11. *Idem.*, *J. Phys. D: Appl. Phys.* **9** (1986) 1785.
12. A. J. TWAROWSKI, *J. Chem. Phys.* **77** (1982) 5840.
13. Y. SADAOKA, T. A. JONES and W. GOPEL, *J. Mater. Sci. Lett.* **8** (1989) 1095.
14. A. K. HASSAN and R. D. GOULD, *Int. J. Electron.* **74** (1993) 59.
15. E. H. RHODERICK and R. H. WILLIAMS, "Metal-Semiconductor Contacts," 2nd ed. (Oxford University Press, Oxford, 1988).
16. A. K. GHOSH and T. FENG, *J. Appl. Phys.* **44** (1973) 2781.
17. A. S. RIAD, S. M. KHALIL and S. DARWISH, *Thin Solid Films* **249** (1994) 219.
18. W. WILSON and R. A. COLLINS, *Sensors and Actuators* **12** (1978) 389.
19. G. D. SHARMA, *Synthetic Metals* **74** (1995) 227.
20. J. G. SIMMONS, *J. Phys. D* **38** (1971) 2378.
21. F. R. FAN and L. R. FAULKNER, *J. Chem. Phys.* **69** (1978) 3334.

Received 8 September
and accepted 11 November 2004